Metrol. Meas. Syst., Vol. XVIII (2011), No. 1, pp. 105-114

PAN POLSKA AKADEMIA NAUK

METROLOGY AND MEASUREMENT SYSTEMS

Index

www.metrology.pg.gda.pl

M&MS

SURFACE ROUGHNESS ANALYSIS IN MILLING OF TUNGSTEN CARBIDE WITH CBN CUTTERS

Paweł Twardowski

Poznan University of Technology, Faculty of Mechanical Engineering, ul. Piotrowo 3, 60-965 Poznan, Poland (✉pawel.twardowski@put.poznan.pl)

Abstract

In this paper, an experimental surface roughness analysis in milling of tungsten carbide using a monolithic torus cubic boron nitride (CBN) tool is presented. The tungsten carbide was received using direct laser deposition technology (DLD). The depth of cut (a_p), feed per tooth (f_z) and tool wear (VB_c) influence on surface roughness parameters (*Ra*, *Rz*) were investigated. The cutting forces and accelerations of vibrations were measured in order to estimate their quantitative influence on *Ra* and *Rz* parameters. The surface roughness analysis, from the point of view of milling dynamics was carried out. The dominative factor in the research was not feed per tooth f_z (according to a theoretical model) but dynamical phenomena and feed per revolution *f* connected with them.

Keywords: milling, tungsten carbide, CBN, surface roughness, dynamics.

1. Introduction

Tungsten carbide has excellent physicochemical properties such as superior strength, high hardness, high fracture toughness and high abrasion wear-resistance. These properties impinge wide application of tungsten carbide in industry for cutting tools, molds and dies.

The most popular method for producing tungsten carbide components is by powder metallurgy technology. Nonetheless, for individual, small quantity production or product prototyping this method is too costly and time consuming. The alternative to powder metallurgy is Direct Laser Deposition (DLD) technology, which can be used to quickly produce metallic powder prototypes by a layer manufacturing method [1, 2].

Direct Laser Deposition is an extension of the laser cladding process, which enables three-dimensional fully-dense prototype building by cladding consecutive layers on top of one another [3].

DLD technology is increasingly being used in production of functional prototypes, to modify or repair components which have excellent hardness, toughness and abrasion wear-resistance. In the near future DLD technology will be used in manufacturing of spare parts in long term space missions [4] or submarine applications [5].

Presently, most components produced by DLD technology have unsatisfactory geometric accuracy as well as surface roughness and require some post-process machining to finish them to required tolerances [6].

Recently tendencies are seen to machine brittle materials, such as tungsten carbide and silicon carbide, by a superhard CBN (cubic boron nitride) and PCD (polycrystalline diamond) cutters in cutting conditions assuring ductile cutting [7 – 9]. The authors of paper [7] have investigated CBN tool wear in milling of tungsten carbide. According to their research machined surface roughness shows insignificant change with the progress of the tool flank wear. In the papers [8, 9] theoretical analyses on the ductile cutting of the tungsten carbide

Article history: received on Oct. 19, 2010; received in revised form on Jan. 18, 2011; accepted on Feb. 9, 2011; available online on Mar. 21, 2011; DOI: 10.2478/v10178-011-0010-7.

workpiece in relation to the temperature, hardness and fracture toughness of the workpiece material were carried out. The investigation indicated that in the cutting of tungsten carbide there is a transition between ductile chip formation and brittle chip formation. The transition depends on the tool geometry, the workpiece material and the cutting condition.

Geometric accuracy is very often understood as surface roughness, defined by parameters *Ra* and *Rz* according to ISO 4287:1984. One of the most significant conditions influencing surface roughness is feed (for conventional workpiece materials such as steels and non-ferrous metals). The increase of feed per tooth f_z leads to an increase of surface roughness. Many authors indicate that cutting speed v_c is also a very important parameter influencing surface microroughness.

Discussing the most important conditions influencing surface roughness, the influence of process dynamics should be also taken into account. The process dynamics is mostly characterized by the forces and vibrations. Vibrations in a machining process are caused by many various parameters e.g. for rotational elements (mill), even the smallest tool-spindle subsystem unbalance generates a centrifugal force which increases with rotational speed increase. Therefore very often the dominative factor influencing surface roughness is not feed per tooth f_z, but feed per revolution f connected with rotational speed n.

The present state of knowledge related to surface roughness generated in the machining process primarily applies to conventional materials. Machining of tungsten carbide is a relatively novel process. Therefore the number of works connected with this problem is comparatively small, and tungsten carbide cutting ability is still insufficiently examined.

2. Research range and method

The main purpose of the work was surface roughness analysis in milling of tungsten carbide using monolithic torus cubic boron nitride (CBN).

Tungsten carbide obtained through direct laser deposition technology (DLD – see Fig. 1) was used as the machined workpiece in this study. In this research a 2–toothed cubic boron nitride monolithic torus end mill was used. Tool diameter was d = 12 mm, corner radius was r_ε = 0.5 mm, cutting edge inclination angle was $\lambda_s = 0^0$ and the radius of tool arc cutting edge was r_n = 4 μm (see Fig. 2). The cutting tests were conducted in face milling conditions on 5–axis DECKEL MAHO model DMU 60monoBLOCK milling center. The research range is depicted in Table 1. Two series of cutting tests were performed. In the first series the tool wear for two different cutting speeds was examined. This series also included the measurement of surface roughness parameters. In the second series surface roughness parameters were measured for all combinations of feed per tooth f_z and depth of cut a_p.

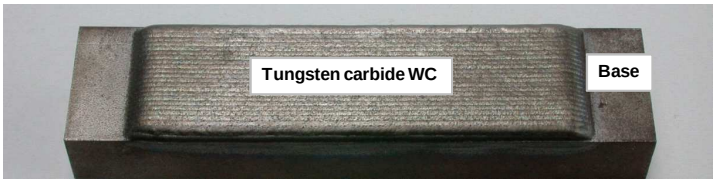

Fig.1. The machined sample

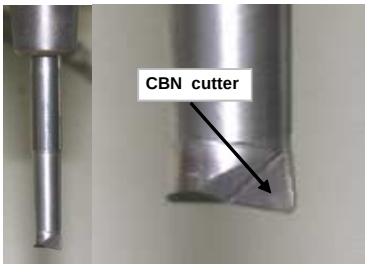

Fig. 2. CBN end mill applied in the research

CBN torus end mill applied in the research had a corner radius r_ε = 0.5 mm, while the axial depth of cut was a_p = 0.02 mm, which indicates that the corner radius was 25 times

greater than the depth of cut. Therefore the CBN tool cut the material by its face part (see Fig. 3) instead of the cylindrical one.

Tool wear determined by the VB_c indicator was measured after each pass (length of one pass – length of the sample L_f = 20 mm) on the optic microscope with 0.01mm scale interval, according to the scheme depicted in Fig. 4.

Table 1. Research range

Series I							
No.	cutting speed v_c [m/min]	rotational speed n [rev/min]	feed per tooth f_z [mm/tooth]	feed rate v_f [mm/min]	axial depth of cut a_p [mm]	radial depth of cut a_e [mm]	tool wear VB_c [mm]
1	68	1800	0.05	180	0.02	6	< 0.4
2	150	3980		398			
Series II							
No.	a_p [mm]	f_z [mm/tooth]		v_c [m/min]	a_e [mm]	VB_c [mm]	
1	0.010	0.025; 0.05; 0.075; 0.1		68	6	< 0.05	
2	0.015	0.025; 0.05; 0.075; 0.1					
3	0.020	0.025; 0.05; 0.075; 0.1					

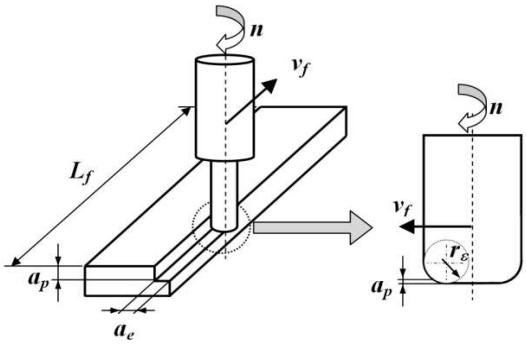

Fig. 3. Schematic illustration of face milling process and the view of the sample

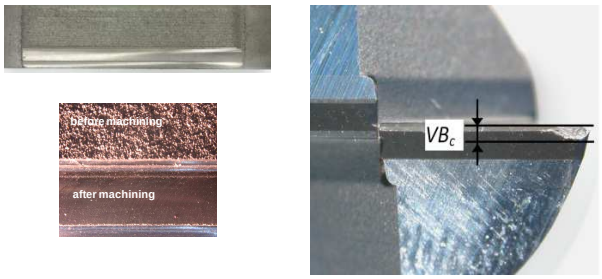

Fig. 4. Tool wear measurement

All the surface roughness measurements were carried out on the machined surface after the face milling process. Three-dimensional (3D) measurements [10 – 13] were achieved using a stationary profilometer Hommelwerke T8000. Two dimensional measurements were made by a T500 profilometer (Hommelwerke), equipped with T5E head and Turbo DATAWIN software. The sampling length lr = 0.8 mm, the evaluation length $ln = 5 \cdot lr$ = 4.0 mm, the length of cut–off wave λc (cut–off) = 0.8 mm and an ISO 11562(M1) filter were applied. After each pass the surface roughness was measured parallel to the v_f vector (feed rate – see Fig. 3). As a result of 2D measurements the surface profile charts were obtained. On the basis of surface profile charts the *Ra* and *Rz* parameters were calculated using Turbo Datawin-NT software.

Parallel to the tool wear measurements, the cutting force and acceleration of vibration components were measured (in the machine tool coordinates – see Fig. 5), in the following directions: direction X – feed normal force measurement F_{fN} [N], direction Y – feed force measurement F_f [N], direction Z – thrust force measurement F_p [N], and direction X – acceleration of vibrations in the feed direction A_f [m/s^2], direction Y – acceleration of vibrations in the feed normal direction A_{fN} [m/s^2], direction Z – acceleration of vibrations in the thrust direction A_p [m/s^2].

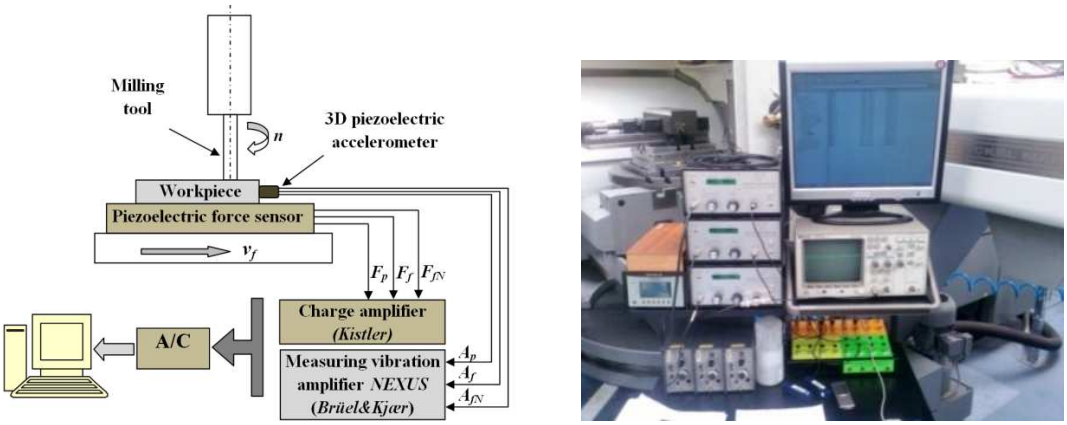

Fig. 5. Block scheme and a view of the cutting force and acceleration of vibrations experimental apparatus

3. Research results and analysis

3.1. Influence of tool wear on surface roughness

As presented in Table 1, the cutting speed v_c and tool wear VB_c were variable in the research. For that reason, in the first place the changes of tool wear in function of cutting time t_s were analyzed (see Fig. 6).

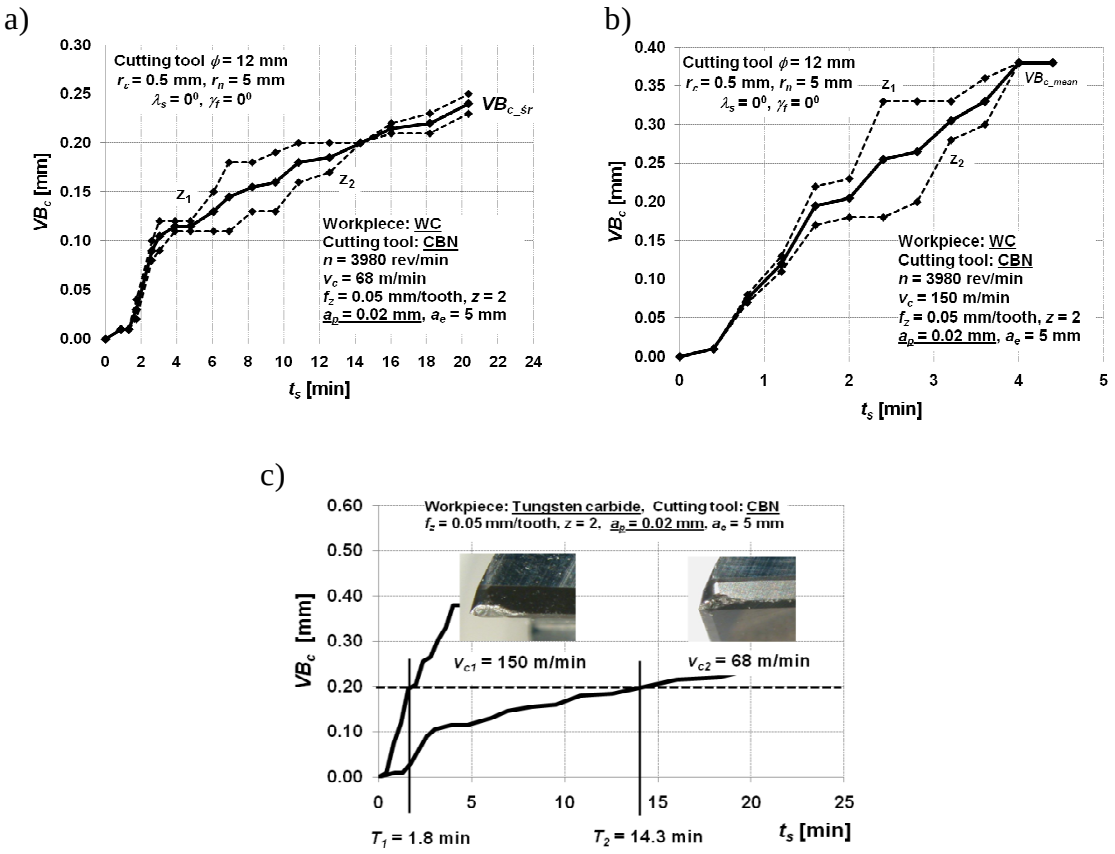

Fig. 6. a), b) Tool wear in function of cutting time t_s for two investigated cutting speeds v_c; c) tool wear comparison for exemplary dullness criterion VB_c = 0.2 mm (z_1, z_2 – number of tooth, T_1, T_2 – tool life)

As it can be seen, the tool wear process for each tooth is similar, i.e. there are no significant deviations of VB_c values for respective teeth. Introducing an arbitrary dullness criterion VB_c = 0.2 mm, it can be seen that a twofold cutting speed v_c increase caused an almost eightfold tool life T decrease. On the basis of acquired data the s exponent used in Taylor`s equation ($T = C_T/v_c^s$, where C_T is constant dependent of workpiece properties) can be estimated, but it is necessary to emphasize that determining the s exponent from two experimental values is not very accurate. After consideration of the v_{c1}, v_{c2}, T_1 and T_2 , the s = 2.65 was obtained. This value is located in the range of the s exponents characteristic for high speed milling of hardened steel, thus the intensity of cutting speed v_c influence on tool life T in tungsten carbide milling is similar to that for hardened steel.

Moreover, the tool wear concentrates on the flank face of the tool (see Fig. 6c). Because of this the relations between the tool wear and both forces and vibrations in the thrust direction were observed (see Fig. 7). The correlation coefficient R^2 for cutting force and vibration components in the feed normal direction – A_{fN} and F_{fN} shows that there is no correlation between the tool wear and RMS values of measured signals. In case of force and vibration thrust direction (A_p, $F_p = f(VB_c)$) a clear relation between tool wear and measured signals was observed. In this case the correlation coefficient R^2 is equal to 0.8 – 0.95, which shows that tool wear has an influence on cutting force and vibration components in the thrust direction. Similar dependencies were observed for a cutting speed of v_c = 150 m/min.

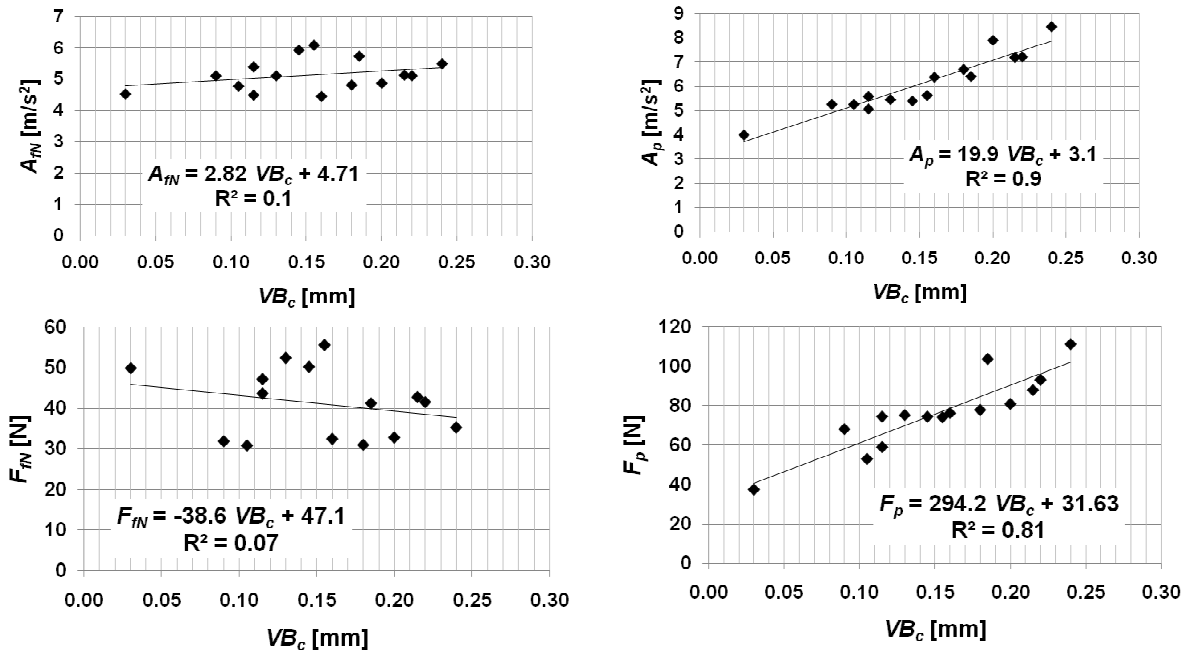

Fig. 7. Comparison of RMS values of cutting force and vibration components in various directions as a function of tool wear (v_c = 68 m/min)

During machined surface generation in face milling, the knowledge about nature and amplitude of forces and vibrations in the thrust direction (orthogonal to the investigated surface) has an essential meaning – particularly signal dynamic variation. Temporary force variation leads to tool corner displacement (along a closed trajectory in the $X – Y$ plane), which propagates directly to the workpiece and thus generating micro–unevenness on the machined surface. The greater tool corner displacements (vibrations) lead to higher micro-unevenness and as a consequence surface roughness parameters.

Unfiltered P-profile and corresponding to them frequency spectra for thrust force F_p are depicted in Fig. 8 and 9.

In case of face milling the thrust force F_p acting in the direction parallel to the height of surface micro–unevenness is highly responsible for surface roughness form and value. From the frequency spectra charts it can be seen that for the thrust force F_p only the spindle speed frequency *fo*, and its second harmonic *2·fo* are dominant (similar dependencies were observed for the other force and vibration directions).

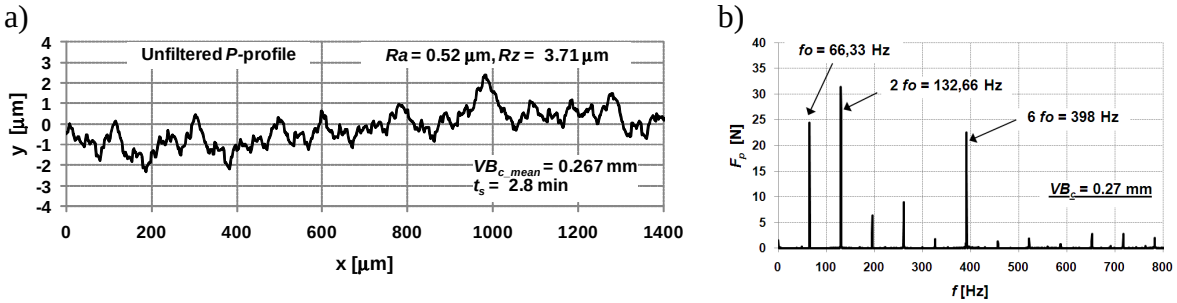

Fig. 8. a) Unfiltered *P*-profile; b) F_p frequency spectrum for v_c = 150 m/min and VB_c = 0.27 mm

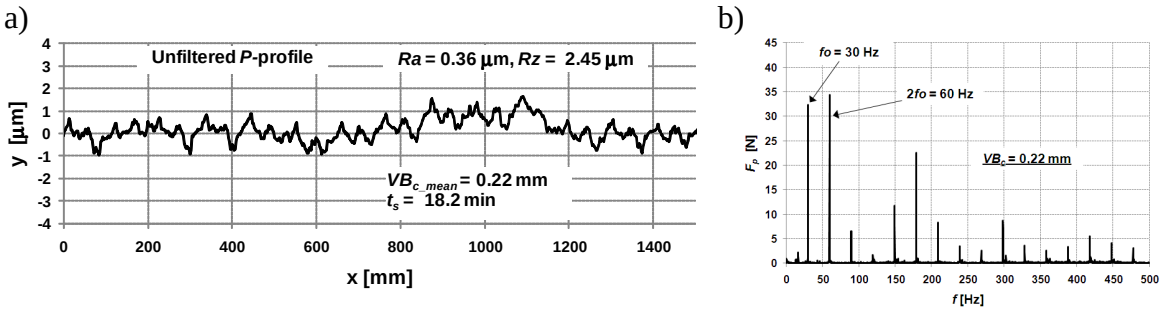

Fig. 9. a) Unfiltered *P*-profile; b) F_p frequency spectrum for v_c = 68 m/min and VB_c = 0.22 mm

In this case (number of teeth z = 2, v_c = 68 m/min, n = 1800 rev/min and $fo = n/60$) the second harmonic *2·fo* overlaps with tooth passing frequency ($2 \cdot fo = z \cdot fo$). For the frequency *fo* = 30 Hz (see Fig. 9) the tool revolution period t is equal to 0.0333s, which at the feedrate v_f = 180 mm/min corresponds to L = 0.1 mm transference. This transference corresponds precisely to feed-per-revolution value f = 0.1 mm/rev, whereas the second harmonic $z \cdot fo$ = 60 Hz is equal to feed per tooth (f_z = 0.05 mm/tooth). The same dependencies were observed for cutting speed v_c = 150 m/min. Since in most frequency spectra *fo* and *z·fo* frequencies are dominant, the principal factors influencing the form of surface roughness could be feed-per-revolution f and feed-per-tooth f_z (as established in Equation 1**).**

This statement is confirmed by 3D surface roughness charts including a Power Density Function analysis (see Fig. 10, 11) on which f and f_z values are clearly visible.

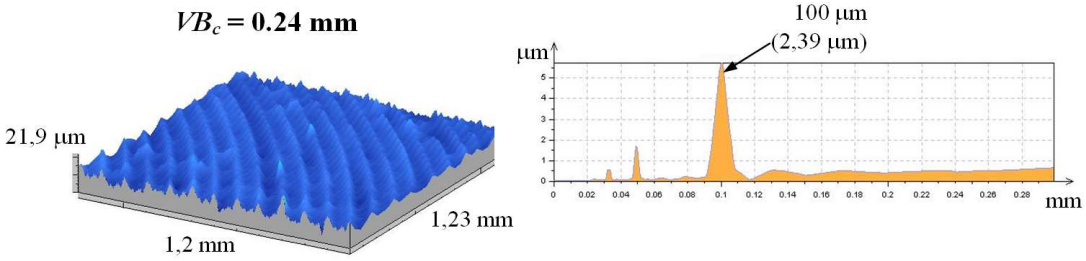

Fig. 10. 3D surface roughness chart for v_c = 68 m/min and corresponding Power Density Function

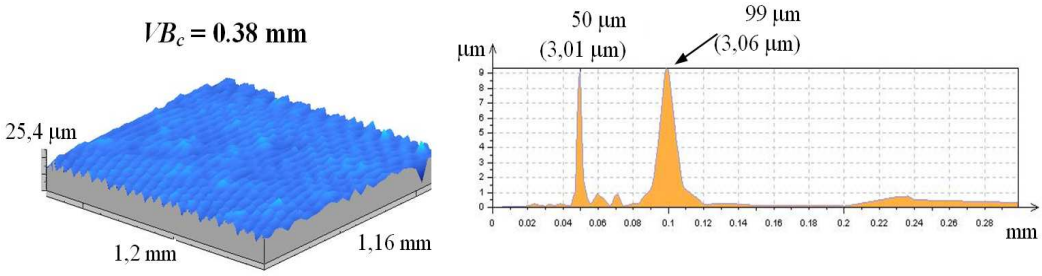

Fig. 11. 3D surface roughness chart for v_c = 150 m/min and corresponding Power Density Function

For the cutting speed v_c = 68 m/min feed-per-revolution f value is dominant (see Fig. 10), and hence its participation in generation of micro-unevenness is higher than that for feed-per-tooth f_z. In the second case (when v_c = 68 m/min – see Fig. 11) the f and f_z participation is comparable and therefore 3D surface roughness charts for investigated cutting speeds have a different form. Cumulative *Ra* and *Rz* parameters charts in function of tool wear VB_c are shown in Fig. 12 and 13.

While in some instances the cinematic – geometric relations were seen, for the whole investigated range (the range of tool wear) no correlation between the surface roughness parameters and tool wear was found. For both analyzed cases (i.e. for v_c = 68 m/min and v_c = 150 m/min) feed per tooth was f_z = 0.05 mm/tooth.

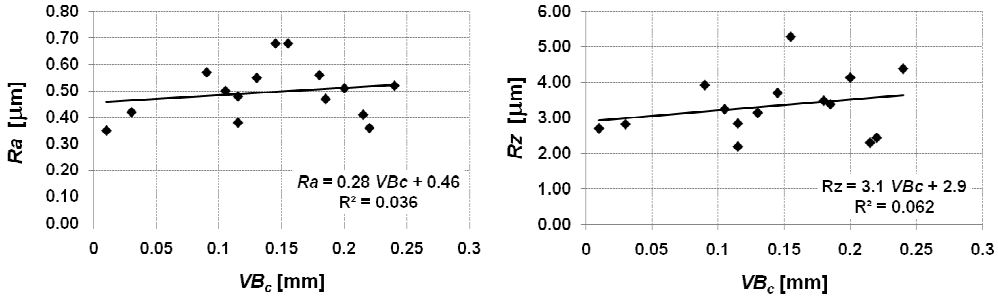

Fig. 12. Surface roughness *Ra* and *Rz* in function of tool wear VB_c for v_c = 68 m/min

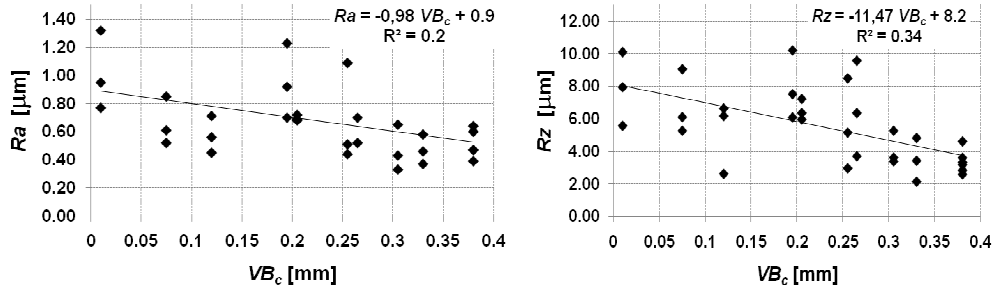

Fig. 13. Surface roughness *Ra* and *Rz* in function of tool wear VB_c for v_c = 150 m/min

The height of theoretical surface roughness can be determined from the following equation [15]:

$$Rt\_max = \frac{f_z^2}{8 \cdot r_\varepsilon} \cdot 1000 \ \ [\mu m] \tag{1}$$

where: *Rt_max* [µm] – theoretical surface roughness,
r_ε [mm] – the cutting edge radius,
f_z [mm/tooth] – feed per tooth.

Using Equation 1 the theoretic surface roughness value *Rt_max* can be calculated, which by assumption should be higher than the *Rz* value. After substituting cutting parameters to Equation 1 the *Rt_max* value equal to 0.625 µm was obtained, while the lowest real surface roughness value was $Rz \approx 2.00$ µm (for $v_c = 150$ m/min and $VB_c = 0.33$ mm). It shows that the theoretical model is very inaccurate.

3.2. Influence of feed-per-tooth f_z and depth of cut a_p on surface roughness

For the second investigated series (see Table 1), the depth of cut a_p and feed-per-tooth f_z were variable. Fig. 14 depicts exemplary profile charts and corresponding to them *Ra* and *Rz* parameters for various feed-per-tooth f_z values. As can be seen, the fourfold feed-per-tooth f_z increase did not make any significant qualitative and quantitative surface unevenness changes. It denotes that feed insignificantly influences surface roughness, which is not in full agreement with the results shown in Fig. 15.

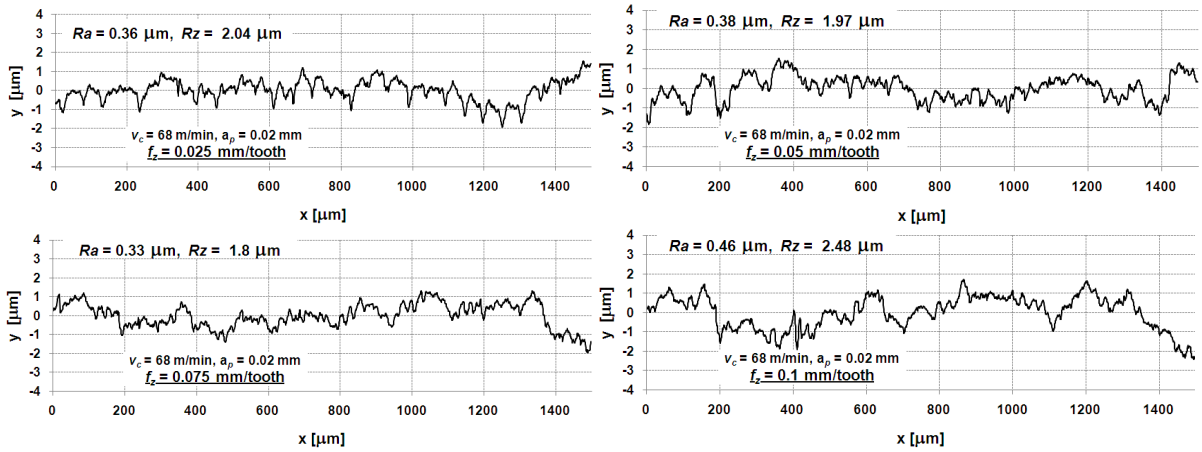

Fig. 14. Exemplary profile charts for various feed per tooth f_z values

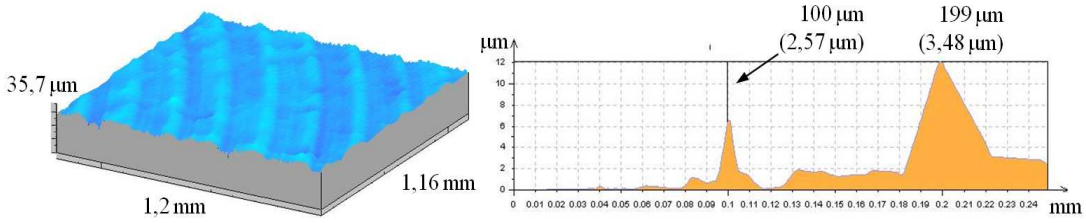

Fig. 15. 3D surface roughness for $v_c = 68$ m/min, $a_p = 0.02$ mm, $f_z = 0.1$ mm/tooth and corresponding Power Density Function

Three dimensional micro-unevenness image shows the cinematic-geometric projection of the cutting edge in the workpiece. It is confirmed by the Power Density Function chart, from which the dominative peak $f_z = 0.1$ mm/tooth is seen.

It turns out that for some instances, a characteristic cinematic-geometric projection of the cutting edge in the workpiece can be seen, however in a wider surface roughness range there is no typical relation. Fig. 16 depicts surface roughness parameters *Ra* and *Rz* (for $v_c = 68$ m/min) in function of feed-per-tooth f_z. From these charts no influence of feed-per-tooth f_z on surface roughness is seen, despite of $f_z = 0.1$ mm/tooth. In this case the theoretic value of *Rzt* is comparable to the real *Rz* value. It is commonly known that the increase of feed-

per-tooth f_z is accompanied by the increase of surface roughness (Equation 1). Theoretically, the lower the feed is fixed a lower surface roughness is generated (see Fig. 16). Nevertheless in practice the differences between theoretical and real surface roughness values are increasing with feed decrease [14, 15].

Similar conclusions can be proposed from cumulative *Ra* and *Rz* charts for all a_p and f_z combinations (see Fig. 17). Twofold a_p and fourfold f_z increase caused insignificant *Ra* and *Rz* change. Therefore in the range of conducted research no unequivocal increase of surface roughness in function of investigated factors was stated.

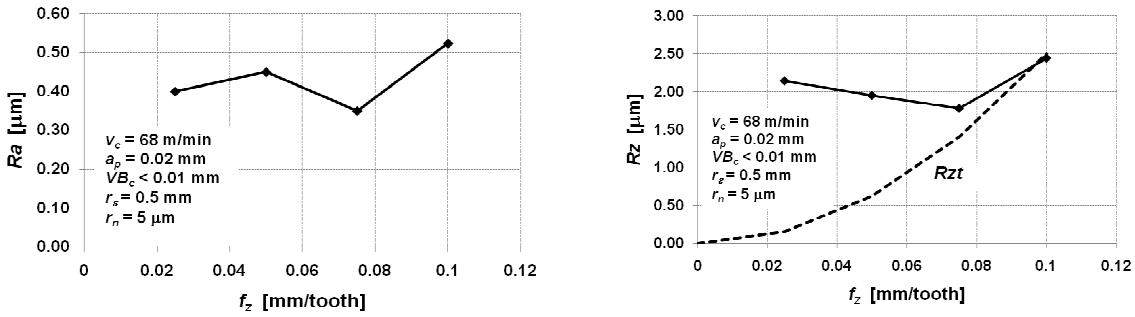

Fig. 16. Surface roughness *Ra* and *Rz* in function of feed per tooth f_z

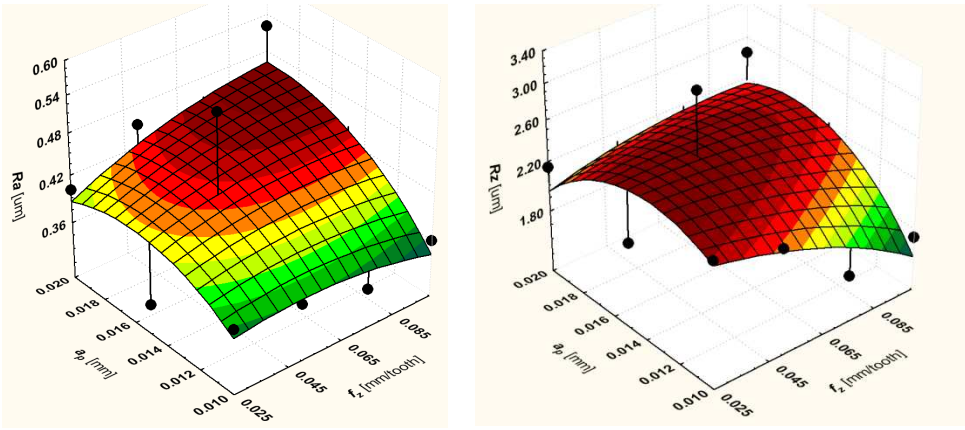

Fig. 17. Surface roughness *Ra* and *Rz* in function of feed per tooth f_z and depth of cut a_p

4. Conclusions

In the range of conducted research no influence of depth of cut a_p, feed-per-tooth f_z and tool wear VB_c on machined surface roughness was found. In the whole tool wear variability range, the surface roughness parameters are changing randomly, independently of cutting speed v_c.

Analysis of force and acceleration of vibration components revealed that dominant spectrum frequencies (*fo* and *zfo*) have direct influence on the form of micro-unevenness, which is confirmed by the Power Density Function analysis.

The comparison of theoretic surface roughness parameters to their real values confirms the well known fact (with reference to e.g. hardened steels) that differences between theoretical and real surface roughness values are increasing with feed decrease.

The milling process of tungsten carbide, in the range of cutting depths several times (3–4 fold) greater than critical depth of cut (corresponding to minimum uncut chip thickness [8, 9]) enables obtaining surface roughness parameters *Ra* similar to those generated in milling on ultraprecision machine tools [7]. It means that in order to obtain relevant machined surface

quality (mainly surface roughness) the application of ultraprecision machine tools is not necessary. Comparable surface roughness parameters one can obtain on less-rigid conventional machine tools.

References

[1] Banerjee, R., Collins, P.C., Genc, A. (2003). Fraser, Direct laser deposition of in situ Ti-6Al-4V-TiB composites. *Materials Science and Engineerin,* A358, 343–349.

[2] Fearon, E., Watkins, K.G. (2004). Optimisation of layer height control in direct laser deposition. *23nd International Congress on Applications of Lasers & Electro–Optics (ICALEO 2004).* San Francisco. California. Laser Institute of America, 597(97).

[3] Murphy M., Lee C., Steen, W. M. (1993). Studies in rapid prototyping by laser surface cladding. *Proceedings of ICALEO*, 882–891.

[4] Taminger, K.M.B., Hafley, R.A., Dicus, D.L. (2002). Solid freeform fabrication: An enabling technology for future space missions. *Proceedings of International Conference on Metal Powder Deposition for Rapid Manufacturing*. San Antonio, 51–60.

[5] Mazumder, J., Choi, J., Schifferer, A. (1999). Direct materials deposition: designed macro– and microstructure. *Materials Research Innovations.* publ. Springer-Verlag, 3(3), 118–131.

[6] Choi, J., Sundaram, R. (2002). A process planning for 5 – axis laser-aided DMD process. *Proceedings of International Conference on Metal Powder Deposition for Rapid Manufacturing*. San Antonio, 112–120.

[7] Liu, K., Li, X.P., Rahman, M., Liu, X.D. (2003). CBN tool wear in ductile cutting of tungsten carbide. *Wear,* 255, 1344–1351.

[8] Liu, K., Li, X.P. (2001). Ductile cutting of tungsten carbide. *Journal of Materials Processing Technology,* 113, 348–354.

[9] Liu, K., Li, X.P. (2001). Modelling of ductile cutting of tungsten carbide. *Trans. NAMRI/SME*, 29, 251–258.

[10] Wieczorowski, M. (2002). Future trends of surface morphology analysis". *Metrology and Measurement Systems*, 9(3), 221–234.

[11] Wieczorowski, M. (2002). Sampling on a spiral for surface topography". *Metrology and Measurement Systems*, 9(3), 195–208.

[12] Wieczorowski, M. (2009). Theoretical basis of morphological filtering in the measurement of surface roughness. *Archiwum Technologii Maszyn i Automatyzacji*, 29(4), 41–49 (in Polish).

[13] Wieczorowski, M., Mrozek, R., Andrałojć, P. (2010). The Use of Surface Asperities Analysis to Investigate Wear of Bodies in Contact on Example of Brake Elements. *Metrology and Measurement Systems*, 17(2), 271-278.

[14] Kawalec, M., Rybicki, M. (2009). Surface texture feature, face milling, hardened steel. *Mechanik,* 10, 779–788 (in Polish).

[15] Kawalec, M. (1980). Physical and technological problems in machining with small cutting thicknesses. *Wydawnictwo Politechniki Poznańskiej,* Seria Rozprawy, 106, Poznań. (in Polish).